

## The view of galaxy formation from Hawaii: Seeing the dark side of the universe.

L.L. Cowie and A.J. Barger

*Institute for Astronomy, University of Hawaii, 2680 Woodlawn Drive, Honolulu, HI 96822*

**Abstract.** The strength of the submillimeter background light shows directly that much of the energy radiated by star formation and AGN is moved to far infrared wavelengths. However, it is only as this background at  $850\ \mu\text{m}$  has been resolved with direct submillimeter imaging that we have seen that it is created by a population of ultraluminous (or near ultraluminous) infrared galaxies (ULIGs) which appear to lie at relatively high redshifts ( $z > 1$ ). Mapping the redshift evolution of this major portion of the universal star formation has been difficult because of the poor submillimeter spatial resolution, but this difficulty can be overcome by using extremely deep cm continuum radio observations to obtain precise astrometric information since the bulk of the brighter submillimeter sources have detectable radio counterparts. However, with this precise position information available, we find that most of the submillimeter sources are extremely faint in the optical and near infrared ( $I \gg 24$  and  $K = 21 - 22$ ) and inaccessible to optical spectroscopy. Rough photometric redshift estimates can be made from combined radio and submillimeter energy distributions. We shall refer to this procedure as millimetric redshift estimation to distinguish it from photometric estimators in the optical and near IR. These estimators place the bulk of the submillimeter population at  $z = 1 - 3$ , where it corresponds to the high redshift tail of the faint cm radio population. While still preliminary, the results suggest that the submillimeter population appears to dominate the star formation in this redshift range by almost an order of magnitude over the mostly distinct populations selected in the optical-ultraviolet.

### 1. Introduction

The cosmic far infrared (FIR) and submillimeter (SMM) background, which is the cumulative rest frame FIR emission from all objects lying beyond our Galaxy, has recently been detected by the *FIRAS* and *DIRBE* experiments on the *COBE* satellite (Puget et al. 1996; Guiderdoni et al. 1997; Schlegel et al. 1998; Fixsen et al. 1998; Hauser et al. 1998) and found to be comparable to the total unobscured emission at optical/UV wavelengths. This result shows directly that much of the energy released by the totality of star formation and AGN radiation through the lifetime of the universe has been dust absorbed and reradiated into the rest-frame FIR. This in turn implies that, to obtain a full accounting of the history

of the universal star formation, we must turn our attention to this dark side of the universe.

## 2. Resolving the submillimeter background

The first stage in this process is to locate the individual objects giving rise to the background. Resolution of the extragalactic submm background at  $850\ \mu\text{m}$  became possible almost simultaneously with the measurement of the background when the Submillimeter Common User Bolometer Array (SCUBA; Holland et al. 1999) was installed on the 15-m James Clerk Maxwell Telescope (JCMT) on Mauna Kea. SCUBA's sensitivity and area coverage enabled the sources producing the submm background to be directly imaged for the first time. The current count determinations determined from blank field surveys and from cluster lensed fields (Smail, Ivison & Blain 1997; Barger et al. 1998, 1999b; Hughes et al. 1998; Blain et al. 1999; Eales et al. 1999) are shown in Figure 1. Barger, Cowie and Sanders have shown, using optimal fitting techniques combined with Monte Carlo simulations of the completeness of the count determinations, that the cumulative counts are well fit by a power law above 2 mJy. In addition, they showed that, in order to match the background and fit to the very limited (one source!) information at fainter magnitudes from the lensed sample (Blain et al. 1999), a differential source count law

$$n(S) = N_0/(a + S^{3.2}) \quad (1)$$

was reasonable. Here  $S$  is the flux in mJy,  $N_0 = 3.0 \times 10^4$  per square degree per mJy, and  $a = 0.4 - 1.0$  is chosen to match the  $850\ \mu\text{m}$  extragalactic background light. The 95 percent confidence range for the power law index is from 2.6 to 3.9. The extrapolation suggests that the typical SMM source producing the bulk of the background lies at around 1 mJy, and the direct counts show that roughly 30 percent of the  $850\ \mu\text{m}$  background comes from sources above 2 mJy.

Provided only that the redshifts lie near or above  $z = 1$  (see below), the far-infrared (FIR) luminosity is approximately independent of the redshift. Thus, if we assume an Arp 220-like spectrum with  $T = 47\ \text{K}$  (e.g., Barger et al. 1998), the FIR luminosity of a characteristic  $\sim 1$  mJy source is in the range  $4 - 5 \times 10^{11} h_{65}^{-2} L_\odot$  for a  $q_0 = 0.5$  cosmology ( $7 - 15 \times 10^{11}$  for  $q_0 = 0.02$ ). The FIR luminosity provides a measure of the current star formation rate (SFR) of massive stars (Scoville & Young 1983; Thronson & Telesco 1986),  $\text{SFR} \sim 1.5 \times 10^{-10} (L_{\text{FIR}}/L_\odot) M_\odot \text{ yr}^{-1}$ ; a 1 mJy source would therefore have a star formation rate of  $\sim 70 h_{65}^{-2} M_\odot \text{ yr}^{-1}$  for  $q_0 = 0.5$ , placing the 'typical' submm source at or above the high end of extinction-corrected SFRs in optically-selected galaxies (Pettini et al. 1998). If we were to allow the dust temperature to go as low as 30 K,  $L_{\text{FIR}}$  and the corresponding SFR would be  $\sim 4$  times smaller.

## 3. Direct attempts at a redshift distribution

The identification of the optical/near-infrared counterparts to the SCUBA sources is made difficult by the uncertainty in the  $850\ \mu\text{m}$  SCUBA positions and by the intrinsic faintness of the counterparts. Barger et al. (1999c) presented

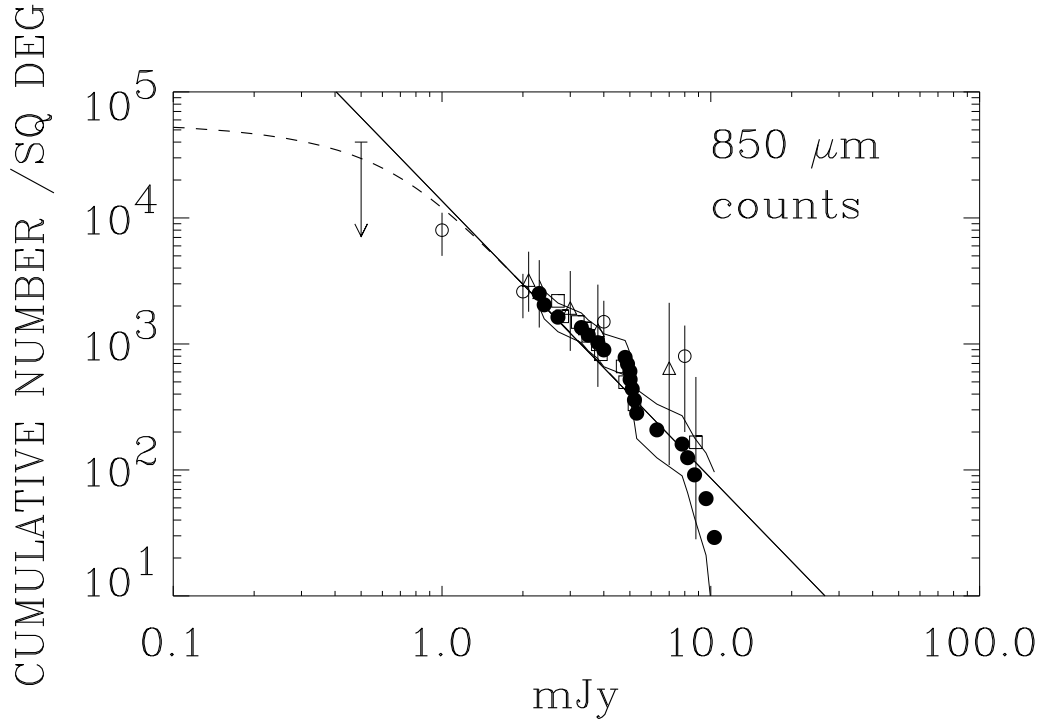


Figure 1. The  $850 \mu\text{m}$  source counts from Barger, Cowie, and Sanders 1999 (solid circles) with  $1\sigma$  error limits (jagged solid lines) are well described by the power-law parameterization in Eq. 1 with  $a = 0.4 - 1.0$ ,  $\alpha = 3.2$ , and  $N_0 = 3.0 \times 10^4 \text{ deg}^{-2} \text{ mJy}^{-1}$  (solid line). The dashed curve shows a smooth extrapolation of this fit to match the EBL measurements using the value  $a = 0.5$ . Counts from Blain et al. (1999) (open circles), Hughes et al. (1998) (open triangles), and Eales et al. (1999) (open squares) are in good agreement with our data and the empirical fit.

a spectroscopic survey of possible optical counterparts to a flux-limited sample of galaxies selected from the 850  $\mu\text{m}$  survey of massive lensing clusters by Smail et al. (1997, 1998). The advantage of a lensed survey is that the clusters magnify any background sources, thereby providing otherwise unachievable sensitivity in the submm, and easing spectroscopic follow-up in the optical. In the Barger et al. survey, identifications were attempted for all objects in the SCUBA error-boxes that were bright enough for reliable spectroscopy; redshifts or limits were obtained for 24 possible counterparts to a complete sample of 16 SCUBA sources. The redshift survey produced reliable identifications for six of the submm sources: two high redshift galaxy pairs (a  $z = 2.8$  AGN/starburst pair (Ivison et al. 1998) and a  $z = 2.6$  Lyman-break-like pair (Ivison et al. (1999)), two galaxies showing AGN signatures ( $z = 1.16$  and  $z = 1.06$ ), and two cD galaxies (cluster contamination). The galaxy pairs were later confirmed as the true counterparts through the detection at their redshifts of CO emission in the millimeter (Frayer et al. 1998, 1999). Because AGN are very uncommon in optically selected spectroscopic samples, it is also probable that the AGN identifications are correct, and they place a rough lower limit of about 20 percent on the fraction of the submillimeter sources which have AGN characteristics. These results suggest that, excluding the cluster objects, about a quarter of the submillimeter sources can be spectroscopically identified.

However, two of the submillimeter sources in the sample have no counterparts to  $I$  around 26 and, while the remaining eight sources have optical galaxies within the large error circles, these are rather normal objects which may simply be chance projections. We shall show in the next section that this is very probably the case. These missing sources may be at higher redshifts, or be more dust obscured, than the spectroscopically identifiable sources. Furthermore Smail et al. (1999), using deep near IR and optical imaging of the fields, have recently detected two extremely red objects which may be the counterparts of two of these sources, rather than the nearby bright spiral galaxies which Barger et al. observed as the most likely counterparts to the SMM sources. This result also suggests that many of the optical source identifications may be suspect.

#### 4. Positional determination from cm continuum radio observations

To proceed further we need accurate astrometric positions, and these are most easily obtained using cm radio continuum observations. Because of the well known radio-FIR correlation, both the cm data and the submillimeter observations are linearly dependent on the star formation rates in the galaxy (Condon 1992), though the ratio of the 850  $\mu\text{m}$  flux to the cm radio flux rises rapidly as a function of redshift because of the opposite signs of the K-correction in the two wavelength ranges. (We discuss this further in the next section.) Because of the redshift dependence, a cm flux-limited sample will contain a high proportion of lower redshift objects, while the 850  $\mu\text{m}$  sample will choose out primarily the high redshift objects.

The flanking field region of the Hubble deep field (the HFF) is well suited to looking at the radio versus submillimeter selection. Eric Richards (1999) has recently obtained an extremely deep VLA 20 cm image of this region, with a relatively uniform ( $1\sigma = 8\mu\text{Jy}$ ) sensitivity over the whole flanking field region,

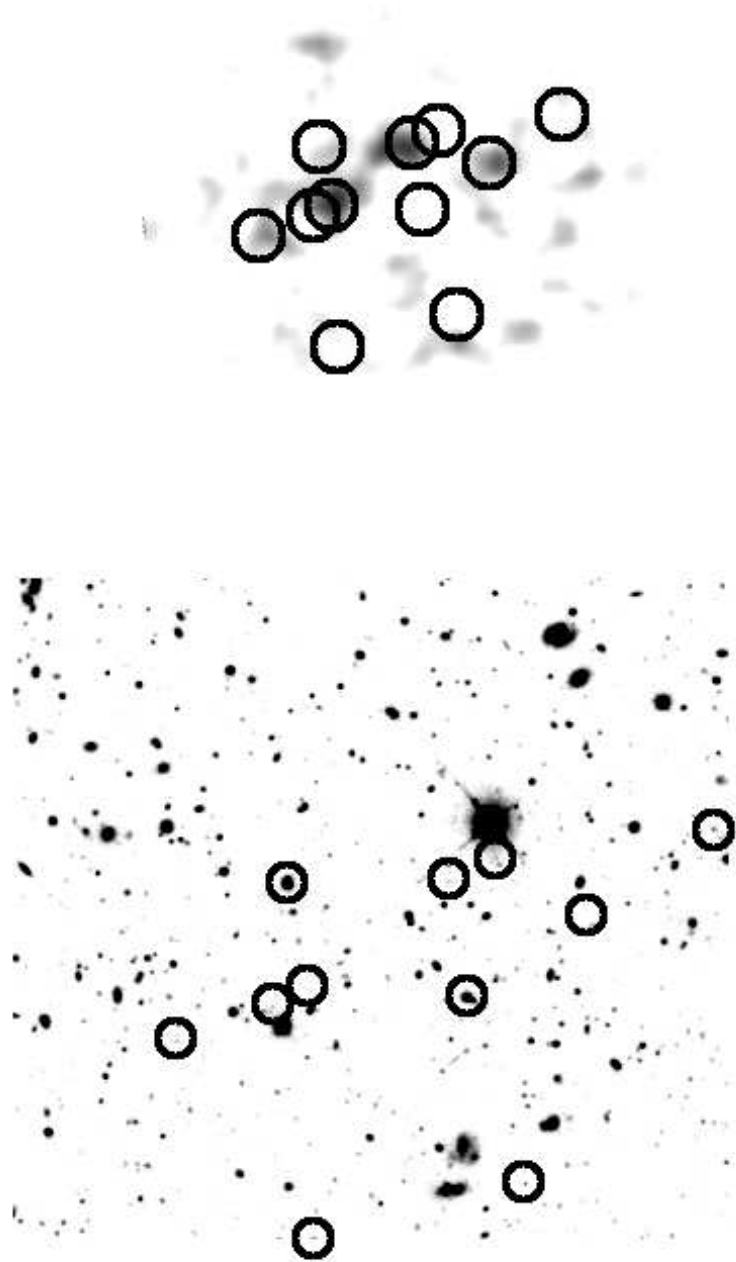


Figure 2. Radio sources in the HFF: the figure shows an overlay of the 20 cm radio sources in a small region of the HFF on a SCUBA 850  $\mu\text{m}$  image on the top and on a near IR image of the region on the bottom. (N is to the right and E to the top in these images.) In general it is the radio sources which are faint in the optical and near IR that are detected in the submillimeter.

which can be combined with the deep ground based optical and near IR (NIR) imaging of the HFF (Barger et al. 1999a). Richards et al. (1999c) find that roughly two thirds of the  $5\sigma$ -selected 20 cm population have relatively bright optical/NIR counterparts while the remaining third are very faint. Barger, Cowie, and Richards (1999) have observed a complete subsample of the radio-selected objects with the LRIS on the Keck II 10m telescope, and find that nearly all the objects with  $K < 20$  can be spectroscopically identified, with a maximum redshift of around 1.2; however, almost none of the fainter objects were identified.

From a total sample of 70 radio selected galaxies in the HFF region, Barger et al. (1999c) chose the 16 with  $K > 21$  for followup with SCUBA. However, because they used the jiggle map mode which provides approximately a 5 square arcminute field around the target, a large fraction of the remaining radio sources (35/54) were also serendipitously measured. 14 of the 16 targeted blank field sources were observed. Even with relatively shallow SCUBA observations ( $3\sigma = 6$  mJy at  $850 \mu\text{m}$ ) a very large fraction of the blank field radio sources were detected in the submillimeter, as is illustrated in Figure 2. Of the 14 targeted sources, 5 are detected above 6 mJy while by contrast none of the 35 optical/NIR bright sources were detected. In the observed fields, which covered slightly more than half of the HFF, a further two sources brighter than 6 mJy were discovered which were not in the radio sample. Even if there are further non-radio-detected submillimeter sources at the same level in the remaining unobserved portions of the HFF, it appears that the radio selection is turning up the majority of the bright submillimeter sources.

The fact that many of the bright submillimeter sources can be identified with the optical/NIR faint radio sources in this way has the extremely important corollary that many of the  $850 \mu\text{m}$ -selected sources have extremely faint optical/NIR counterparts. This is illustrated in Figure 3, where we show the  $K$  and  $I$  magnitudes of radio-selected sources in the HFF, and also in the SSA13 field (Richards et al. 1999c and references therein) where a similar submillimeter survey has been carried out (Cowie, Barger, and Richards 1999). Extremely deep  $K$  observations with NIRC on the Keck I 10m can yield detections of nearly all the  $850 \mu\text{m}$  detected radio sources, and these are found to lie in the  $K = 21 - 22$  range. However, many of the sources are not detected in the  $I$  band at the  $2\sigma$  limit of  $I = 25$  for the HFF, and, for the HDF850.2 source in the HDF proper (Hughes et al. 1998), the source is not seen to  $I = 29$ . The brightest sources lie in the  $I = 24 - 25$  range.

## 5. Millimetric redshift estimation

While it is clear from the work described in section 3 that a fraction of the submillimeter sources have optical and NIR counterparts that are bright enough for spectroscopic identification, the results of section 4 show that a very large fraction simply cannot be identified in this way. At the current time the small numbers of objects suggest that perhaps a quarter of the sources (of which a fairly large fraction have AGN characteristics) are bright in the optical and spectroscopically identifiable, while the remainder fall into the optical/near IR faint category. For this latter category of objects we will have to rely on photometric estimates using the shape of the spectral energy distribution in the radio and

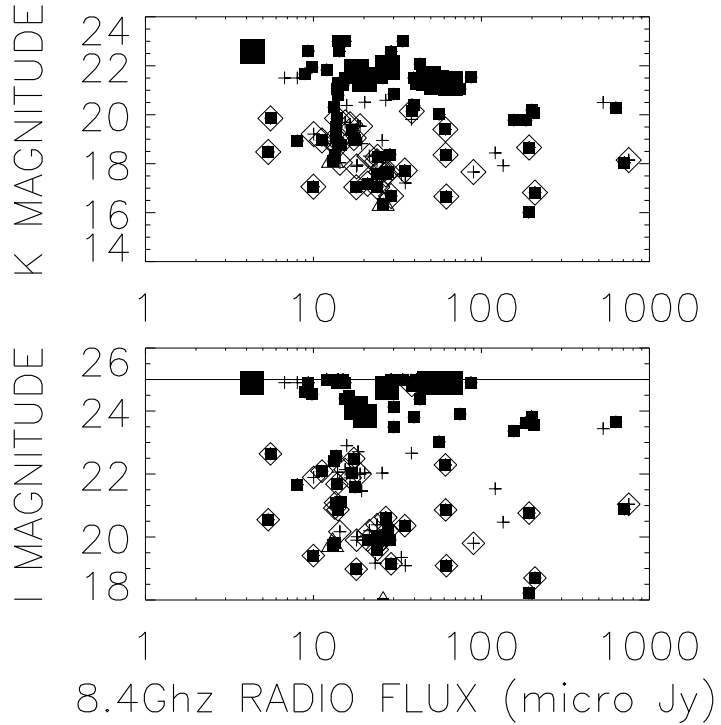


Figure 3. The optical and NIR magnitudes of the radio sources in the HFF and the SSA13 field versus 8.4GHz flux: the whole radio population is shown as crosses with sources which only have 20 cm fluxes extrapolated to 8.4GHz assuming a synchrotron spectrum. Sources with known redshifts are shown with open diamonds and all lie at  $z < 1.2$  except for two quasars in the SSA13 field (Windhorst et al. 1995) which are shown as triangles. Sources which have been observed in the 850  $\mu\text{m}$  but not detected at the typical 6 mJy ( $3\sigma$ ) level are shown as the small squares while those detected at 850  $\mu\text{m}$  are shown as the large squares.

submillimeter, and the submillimeter to NIR ratios (Carrilli and Yun 1999, Blain et al. 1999).

Carrilli and Yun have suggested the use of the 850  $\mu\text{m}$  to 20 cm flux ratio as such a redshift indicator. Because of the opposing spectral slopes of the synchrotron spectrum in the radio and the black body spectrum in the submillimeter, the submillimeter to radio ratio rises extremely rapidly with redshift, as is shown in Figure 4, which is taken from Barger, Cowie, and Richards (1999) where a much more extensive discussion may be found. The primary uncertainty in this quantity lies in the dust temperature dependence, which in the local ULIG sample produces a range in the ratio of about a multiplicative factor of 2 relative to Arp220.

We can test the estimator in a variety of ways. In Figure 4 we have shown the average submillimeter to radio ratios for the objects in the HFF with known spectroscopic redshifts. While none of these sources is individually detected, the average values are consistent with a null result at low redshifts but a strongly significant positive detection for the sources near  $z = 1$ , which is extremely consistent with the Arp220 ratio. Individual submillimeter sources with spectroscopic identifications are also broadly consistent with the expected ratios, though there is a suggestion that, as might be expected, those with the AGN characteristics have slightly lower ratios, though still within the broad general range.

The optically/near IR faint radio sources in the HFF with submillimeter detections are shown as the horizontal lines in the figure. The redshift estimator places them in the same broad general  $z = 1 - 3$  range as the typical spectroscopically identified sources. (For AGN we may be systematically underestimating the redshifts). Radio sources without 850  $\mu\text{m}$  detections probably lie at lower redshifts while the 850  $\mu\text{m}$  sources without radio counterparts may represent the high end redshift tail.

## 6. Discussion

We can summarise the results as follows. Roughly 30 percent of the 850  $\mu\text{m}$  background is already resolved and the slope of the counts is sufficiently steep (a power law index of  $-2.2$  for the cumulative counts) that only a small extrapolation to fainter fluxes will result in convergence to the background. Thus, the typical submillimeter source contributing to the background seems to be in the 1-2 mJy range. Because of the direct correspondence between flux and luminosity at these wavelengths we may identify the sources with ULIGs or near ULIGs. About a quarter of the sources have optical counterparts which are bright enough to be spectroscopically identified, and a large fraction of these show AGN characteristics, though at least one is an extremely bright pair of Lyman break galaxies. However, many of the remaining sources are extremely faint in the optical and NIR ( $K = 21 - 22$ ). Redshift estimation for these sources using the submillimeter to radio ratios places the bulk of them in the same  $z = 1 - 3$  range as the spectroscopically identified sources.

It is interesting to consider where this population fits in the overall history of the universal star formation. One uncertainty in doing this is the question of what fraction of the SMM light is powered by AGN rather than star formation.



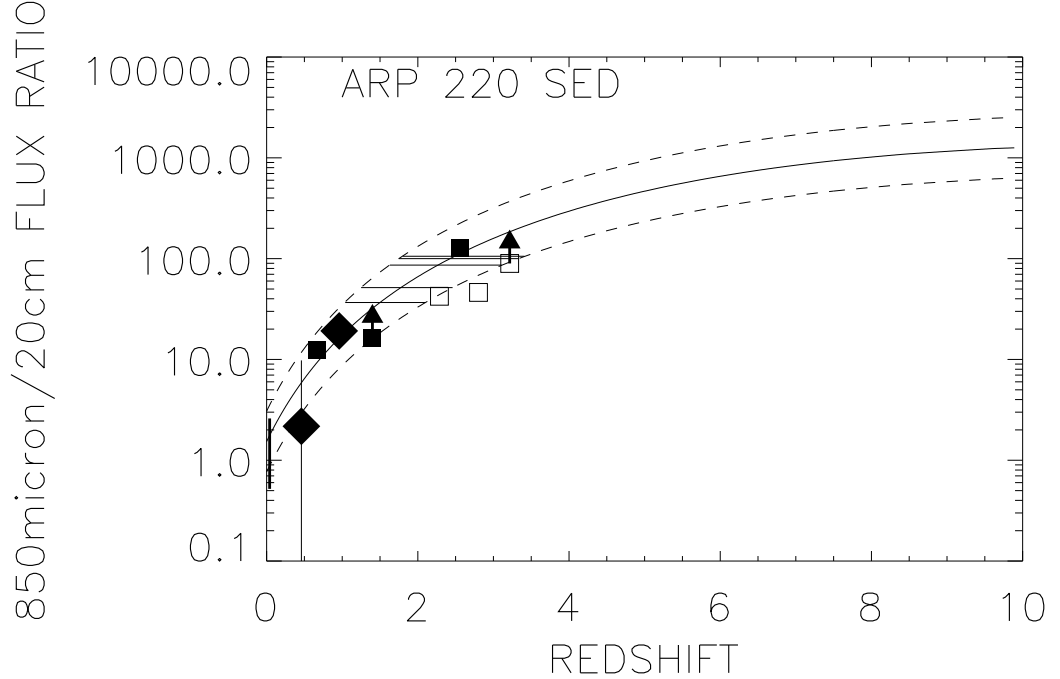


Figure 4. Millimetric redshift estimation: The solid curve shows the ratio of the 850  $\mu\text{m}$  to 20 cm flux that a non evolving ARP220 would have as a function of redshift. The solid bar at low redshift shows the range of the 850  $\mu\text{m}$  fluxes to the 8.4GHz flux at low redshift extrapolated to 20 cm assuming a synchrotron spectrum with the data taken from Rigopoulou et al. (1996). This suggest that the ULIGS have a range of about a multiplicative factor of 2 relative to ARP220 which is shown by the dashed lines. The average submillimeter to 20 cm ratio of the galaxies which have spectroscopic redshifts and also have been observed in the submillimeter are shown as the large diamonds with  $1\sigma$  errors. The lowest point is consistent with a null detection but in the higher redshift bin there is a strong positive detection consistent with an ARP220 ratio. Individually detected objects from Lilly et al. (1999) and Ivison et al. (1999) are also consistent within the error spread though those with AGN characteristics (open symbols) appear to fall low in the figure. The solid line show the best guess for the redshift range (typically  $z = 1 - 3$ ) for the optically/NIR faint galaxies which are detected in the submillimeter. Radio objects which are not detected in the submillimeter are likely to lie at lower redshifts than this while submillimeter detected objects which are not seen in the radio are potentially at higher redshift.

It has long been debated whether the dust-enshrouded local ULIGs are powered by massive bursts of star formation induced by violent galaxy-galaxy collisions or by AGN activity. A recent mid-infrared spectroscopic survey of 15 ULIGs by Genzel et al. (1998) found that 70 – 80 per cent of the sample are predominantly powered by star formation and 20 – 30 per cent by a central AGN. Thus, while the spectroscopic follow-up studies of the gravitationally lensed submm sample (Barger et al. 1999c; Ivison et al. 1998) discussed in section 3 indicate that at least 20 per cent of the sample show some AGN activity, we shall assume in the following discussion that a substantial fraction of the submm light arises from star formation.

Several groups (Smail et al. 1998; Eales et al. 1999; Lilly et al. 1999; Trentham, Blain, & Goldader 1999; Barger, Cowie, & Sanders 1999) have suggested that the submm sources are associated with major merger events giving rise to the formation of spheroidal galaxies. The approximate equality of the optical and submm backgrounds supports this hypothesis; present-day spheroidal and disk populations have roughly comparable amounts of metal density, and thus their formation is expected to produce comparable amounts of light (Cowie 1988). Since the volume density of local ULIGS is very low (approximately  $10^{-6} h_{65}^3 \text{ Mpc}^{-3}$  for objects with bolometric luminosities above  $5 \times 10^{11} h_{65}^{-2} L_{\odot}$  e.g. Sanders and Mirabel 1996) it appears that the star formation rate in this population must have been much higher in the past and have declined very steeply after  $z = 1$ , which may also be consistent with this interpretation. For a cumulative source density of  $4.0 \times 10^4 \text{ deg}^{-2}$  required to reproduce the EBL with 1 mJy sources ( $\langle N \rangle = \text{EBL}/\langle S \rangle$  with  $\langle S \rangle \sim 1 \text{ mJy}$ ) and redshifts in the 1 – 3 range, the average space density is  $5 \times 10^{-3} h_{65}^3 \text{ Mpc}^{-3}$  for a  $q_0 = 0.5$  cosmology ( $10^{-3}$  for  $q_0 = 0.02$ ). This space density is rather insensitive to the upper cut-off on the redshift distribution, dropping by only a factor of  $\sim 2$  or 3 if we extend the volume calculation to  $z = 5$ . For comparison, the space density of present-day ellipticals is about  $10^{-3} h_{65}^3 \text{ Mpc}^{-3}$  (Marzke et al. 1994). Within the still substantial uncertainty posed by the dust temperatures, the estimated star formation rate from submm sources in the  $z = 1 - 3$  range is  $\sim 0.3 h_{65} \text{ M}_{\odot} \text{ yr}^{-1} \text{ Mpc}^{-3}$  for  $q_0 = 0.5$ , which is nearly an order of magnitude higher than that observed in the optical,  $\sim 0.04 h_{65} \text{ M}_{\odot} \text{ yr}^{-1} \text{ Mpc}^{-3}$  (e.g., Steidel et al. 1999) suggesting that at these redshifts it is the submillimeter light which marks the bulk of the star formation.

**Acknowledgments.** We would like to thank our collaborators Eric Richards, Dave Sanders, Ian Smail, Rob Ivison, Andrew Blain and Jean-Paul Kneib.

## References

- Barger, A.J., Cowie, L.L., Sanders, D.B., Fulton, E., Taniguchi, Y., Sato, Y., Kawara, K., Okuda, H. 1998, *Nature*, 394, 248
- Barger, A.J., Cowie, L.L., Trentham, N., Fulton, E., Hu, E.M., Songaila, A., Hall, D. 1999a, *AJ*, 117, 102
- Barger, A.J., Cowie, L.L., Sanders, D.B. 1999b, *ApJ*, 518, L5
- Barger, A.J., Cowie, L.L., Smail, I., Ivison, R.J., Blain, A.W., Kneib, J.-P. 1999c, *AJ*, in press

- Barger, A.J., Cowie, L.L., Richards E.A. 1999, AJ, to be submitted
- Blain, A.W., Kneib, J.-P., Ivison, R.J., Smail, I. 1999, ApJ, 512, L87
- Carilli, C.L., Yun, M.S. 1999, ApJ, 513, L13
- Condon, J.J. 1992, ARA&A, 30, 575
- Cowie, L.L. 1988, in *The Post-Recombination Universe*, N. Kaiser & A.N. Lasenby, Dordrecht: Kluwer, 1
- Cowie, L.L., Barger A.J., Richards E.A. 1999 AJ, to be submitted
- Fixsen, D.J., Dwek, E., Mather, J.C., Bennett, C.L., Shafer, R.A. 1998, ApJ, 508, 123
- Eales, S. et al. 1999, ApJ, 515, 518
- Frayer, D.T., Ivison, R.J., Scoville, N.Z., Yun, M., Evans, A.S., Smail, I., Blain, A.W., Kneib, J.-P. 1998, ApJ, 506, L7
- Frayer, D.T., Ivison, R.J., Scoville, N.Z., Evans, A.S., Yun, M., Smail, I., Barger, A.J., Blain, A.W., Kneib, J.-P. 1999, ApJ, 514, 13L
- Genzel, R. et al. 1998, ApJ, 498, 579
- Guiderdoni, B., Bouchet, F.R., Puget, J.-L., Lagache, G., Hivon, E. 1997, Nature, 390, 257
- Hauser, M.G. et al. 1998, 508, 25
- Holland, W.S. et al. 1999, MNRAS, 303, 659
- Hughes, D.H. et al. 1998, Nature, 394, 241
- Ivison, R., Smail, I., Le Borgne, J.-F., Blain, A.W., Kneib, J.-P., Bézecourt, J., Kerr, T.H., Davies, J.K. 1998, MNRAS, 298, 583
- Ivison, R. et al. 1999, MNRAS, submitted.
- Lilly, S.J. et al. 1999, ApJ, 518, 641
- Marzke, R.O., Geller, M.J., Huchra, J.P., Corwin, Jr., H.G. 1994, AJ, 108, 437
- Pettini, M., Kellogg, M., Steidel, C.C., Dickinson, M., Adelberger, K.L., Giavalisco, M. 1998, ApJ, 508, 539
- Puget, J.-L., Abergel, A., Bernard, J.-P., Boulanger, F., Burton, W.B., Desert, F.-X., Hartmann, D. 1996, A&A, 308, L5
- Richards, E.A., Kellermann, K.I., Fomalont, E.B., Windhorst, R.A., Partridge, R.B. 1998, AJ, 116, 1039
- Richards, E.A. 1999a, ApJ, 513, 9L
- Richards, E.A. 1999b, ApJ, in press
- Richards, E.A., Fomalont, E.B., Kellermann, K.I., Partridge, R.B., Windhorst, R.A., Cowie, L.L, Barger, A.J. 1999c, ApJ, submitted
- Rigopoulou, D., Lawrence, A., Rowan-Robinson, M. 1996, MNRAS, 278, 1049
- Sanders, D.B., Mirabel, I.F. 1996, ARA&A, 34, 749
- Schlegel, D.J., Finkbeiner, D.P., Davis, M. 1998, ApJ, 500, 525
- Scoville, N., Young, J.S. 1983, ApJ, 265, 148
- Smail, I., Ivison, R.J., Blain, A.W. 1997, ApJ, 490, L5
- Smail, I., Ivison, R.J., Blain, A.W., Kneib, J.-P. 1998, ApJ, 507, 21L
- Smail, I., Ivison, R.J., Kneib, J.-P., Cowie, L.L., Blain, A.W., Barger, A.J., Owen, F.N., Morrison, G.E. 1999, MNRAS, in press, [astro-ph/9905246]

- Steidel, C.C., Adelberger, K.L., Giavalisco, M., Dickinson, M., Pettini, M. 1999, [astro-ph/9811399]
- Thronson, H.A., Telesco, C.M. 1986, ApJ, 311, 98
- Trentham, N., Blain, A.W., Goldader, J. 1999, MNRAS, 305, 61
- Windhorst, R.A., Fomalont, E.B., Kellermann, K.I., Partridge, R.B., Richards, E., Franklin, B.E., Pascarella, S.M., Griffiths, R.E. 1995, Nature, 375, 471